Recording of continuous cooling precipitation diagrams of aluminium alloys

Benjamin Milkereit [a],[*], Olaf Kessler [a], Christoph Schick [b]

[a] University of Rostock, Faculty of Mechanical Engineering and Marine Technology, 18051 Rostock, Germany
[b] University of Rostock, Inst. of Physics, 18051 Rostock, Germany

ARTICLE INFO

ABSTRACT

The purpose of this report is to present a methodology to record continuous cooling precipitation (CCP) diagrams over the complete range of technical interesting cooling rates for some aluminium wrought alloys. With the information out of CCP-diagrams, the quenching step of the heat-treatment process "Age Hardening" can be optimized. The nanosized precipitations were detected via Differential Scanning Calorimetry (DSC) by identifying their exothermal heat. Aluminium wrought alloy EN AW-6005A was age hardened in three different DSCs whereby cooling rate range varies over 3 orders of magnitude. With increasing cooling rate, the precipitation heat is decreasing. The CCP-diagram covers cooling rates form close to equilibrium conditions at 0.1 K/min up to the critical cooling rate at 375 K/min where the precipitation reaction is suppressed completely. The DSC delivers a very useful method to record full range CCP-diagrams of aluminium alloys. Opposite to other possible methods, it also delivers a measure for the amount of the nanosized precipitates by the amount of released heat. A strategy is presented for the deconvolution of overlapping DSC-peaks.

© 2009 Elsevier B.V. All rights reserved.

1. Introduction

For the strengthening of suitable aluminium alloys a heat-treatment, which is called age hardening is performed. Thereby strength is increased by the mechanism of particle strengthening. The particles, which cause the strengthening, have a typical size in the nanometre-scale. Age hardening contains out of three steps: solution annealing, quenching and aging. During the solution annealing, the relevant alloying elements are dissolved in a solid solution. This state is frozen by quenching and a supersaturated solid solution (SSS) results. In a third step the material is aged, naturally (at room temperature) or artificially (temperatures usually up to 200 °C), for a certain time to get a controlled precipitation of strengthening particles. The precipitation process follows an alloy specific sequence. Maximum strength is reached, when precipitate size and structure hinder dislocation movement most efficiently. These strengthening particles are very small compared to the incoherent equilibrium-phase particles [1].

When an age-hardening aluminium alloy is solution annealed and afterwards cooled too slowly, a precipitation reaction occurs already during cooling. This reaction must be eliminated completely to reach maximum strength during the following aging. Therefore cooling must be done as fast as needed to suppress precipitation. On the other hand cooling should be done as slow as possible to avoid extensive residual stresses and distortions. In order to fit those opposite requirements cooling should be done just above the critical cooling rate, which is the slowest cooling rate where no precipitation reaction occurs. The influence of the cooling rate on the precipitation behaviour is described by continuous cooling precipitation (CCP) diagrams. This information can be used to optimize the quenching step of the age-hardening process. Furthermore, simulation of precipitation during the cooling step out of the age-hardening process is impossible without CCP-diagrams. However, for aluminium alloys only very few CCP-diagrams exist because common procedures to record such diagrams for steels, like dilatometry, are not usable for aluminium alloys. One significant difference between steel and aluminium alloys is that during the comparable heat treatment of steels usually phase transformations with large volume changes take place. For aluminium alloys the matrix phase is constant and only alloying elements (which are typically only few wt.%) precipitate out of the matrix. Hence, the volume effects are much smaller at aluminium alloys.

The precipitation reactions during cooling of solution annealed heat-treatable aluminium alloys are exothermic. Recently it was reported that this precipitation reaction can be detected by Differential Scanning Calorimetry (DSC) in a cooling rate range from 5 K/min to 475 K/min. It was found that with increasing cooling rate the precipitation heat decreases. Consequently, the released heat has been established as a measure for the amount of precipitated particles [2–5,18].

Cavazos and Colas [6] also used the fact that the precipitation is exothermic. They measured precipitation during cooling with a special (Jominy) end-quench test by which several additional thermocouples were placed at the middle axis of the cylindrical sample.

* Corresponding author. Tel.: +49 381 498 9486; fax: +49 381 498 9472.
E-mail address: benjamin.milkereit@uni-rostock.de (B. Milkereit).

This method could implement many sources of error like that this is not a closed system. Additionally the end-quench causes non-linear cooling. The presented CCP-diagram of aluminium alloy 6063 covers a cooling rate range of approximately 2100–35 K/min. Moreover, no direct measure for the amount of precipitates was reported. Li et al. [7] measured continuous cooling precipitation curves of an Al–Cu–Li alloy. Amongst other methods they used the change of electric resistance to follow precipitation during cooling. This method also delivers a large range of cooling rates from approximately 70–1000 K/min. However, no direct measure for the amount of precipitation was reported.

As shown above it is possible to record CCP-diagrams with different methods in different ranges of cooling rates. Until today, no complete CCP-diagrams for aluminium alloys have been published. In order to record complete CCP-diagrams of aluminium alloys the DSC method seems to be most informative because it supplies a measure for the amount of precipitates via the amount of released heat in dependence of cooling rate. However, the mentioned DSC-studies cover only a small range of cooling rates. Nevertheless nowadays scanning calorimetry is possible in a very wide range of cooling rates. Very slow scanning to follow near equilibrium phase changes can be done, beside others, with Heat-Flow-DSCs of the CALVET-type [8]. Ultra fast scanning calorimetry up to 1 MK/s cooling rate is possible with thin film chip calorimeters [9,10]. With the device used by Gao et al. [11] the previously existing gap in heating and cooling rates between ultrafast and conventional DSC is closed now. Even such calorimeters are available, they were not applied to aluminium samples yet because they have to be adjusted to the specific problem. Further the DSC technique is an established method for the investigation of the precipitation sequence during reheating of samples, which are solution annealed and typically quenched in water [12–15]. A review of DSC-work done on aluminium based alloys from 1994 to 2004 is given by Starink [16].

The purpose of this report is to present a method for recording full range CCP-diagrams for low to middle quench sensitive aluminium alloys in the range from very slow cooling near equilibrium (0.1 K/min) to some hundred K/min. The challenges here are relative high temperatures, a wide range of cooling rates and as the most difficult task the detection of the disappearance of the precipitation reaction near the critical cooling rate. To detect the alloy specific critical cooling rate the DSC reaches its limits because of zero released heat when the supersaturated solid solution is obtained completely. The challenge here is to distinguish objectively between a tiny reaction and instrumental noise. An additional problem is the deconvolution of overlapping reaction peaks. Despite the relative big samples, signal smearing is no problem, due to the good thermal conductivity of aluminium. Compared to the research published so far in this field, the developed evaluation method is more objective. It also enables evaluation of the characteristic data in case of overlapping reactions.

2. Materials and methods

The presented investigation was performed with the age-hardening aluminium–magnesium–silicon wrought alloy EN AW-6005A. This is an often-used alloy with middle alloying content. Therefore, a relatively low critical cooling rate was expected. Cylindrical samples were turned from an extruded profile. Samples were turned cylinders with sample masses from 32 to 1550 mg with dimensions from 4 to 6.5 mm in diameter and from 1 to 22 mm in length adapted to cooling rate and calorimeter used. As an inert reference material for the DSC measurements EN AW-1050, pure aluminium with an Al-content of over 99.5 wt.%, was used. The reference samples were turned out of a cast block. The detailed amounts of alloying elements of both materials are shown in Table 1.

Table 1
Alloying elements of the investigated aluminium basis-material: EN AW-6005A and EN AW-1050 (inert reference material).

wt.%	Si	Fe	Cu	Mn	Mg	Cr	Zn	Ti
EN AW-1050	0.09	0.32	0.002	0.004	0.001	0.001	0.01	0.004
EN AW-6005A	0.68	0.20	0.01	0.11	0.57	0.040	0.01	0.018

The samples were solution annealed and cooled in three different types of DSC-devices. An EN AW-1050 reference sample was placed in the reference furnace. Cooling rate varies from very slow cooling (0.1 K/min – equilibrium is expected) in discrete intervals up to critical cooling rate whereby the precipitation is completely suppressed. Selected samples have been artificially aged afterwards. Following hardness testing and metallographic investigations have been performed to confirm the DSC results.

Some conditions were constant for all DSC-experiments:

- Solution annealing temperature and time were 540 °C, 20 min, respectively.
- Excess specific heat capacity was determined from all measurements. That means the difference in specific heat capacity between alloy EN AW-6005A and EN AW-1050. Therefore, a baseline-measurement was done for each cooling rate with EN AW-1050 samples in reference and sample furnaces.
- Measurements were done at ambient pressure.
- Artificially aging was done at 25 °C for 7 min followed by 180 °C for 4 h.

In the cooling rate region above 30 K/min at least three experiments with the same conditions were performed. In the following the average values are shown. At slower cooling fewer experiments were performed because of their long duration.

For each DSC-device, different conditions have been identified to reach optimal results.

The slowest experiments were done with a Heat-Flow-DSC of CALVET-type (Setaram DSC 121). The optimal samples have dimensions of about 5.7 mm in diameter and 21.7 mm in length, which results in a sample mass of approximately 1570 mg. The samples were covered by two standard 300 μl aluminium crucibles with a mass of about 360 mg. Heating was carried out at 5 K/min. The block-temperature was set to 15 °C, but rises up to 30 °C when the furnace reaches the maximum temperature of 540 °C. Cooling power of the circulating bath was not high enough to keep cooling jacket temperature at 15 °C but this is not important for this type of instrument. Cooling rate ranges from 0.05 K/min to 8 K/min.

Cooling rates in the intermediate range from 10 K/min to 30 K/min were performed employing the heat-flow type Mettler DSC 823. The optimal samples for these rates and this device have dimensions of about 5.4 mm in diameter and 1.4 mm in height, which results in a sample mass of approximately 92 mg. The samples were placed in standard aluminium crucibles (49 mg). These crucibles have a positioning pin for exact and equal positioning on the sensing area. The crucibles were tightly closed by a press. Hence, a small hole is to place in the lid in order to avoid buckling of the crucible. Buckling would result from air expansion caused by the large temperature-range. Buckling would disturb the heat flow between sample and sensor. Heating was performed with 30 K/min. A pure nitrogen purge was used. Cooling was realized by a double-stage mechanical cooler.

The fastest used DSC was a Perkin-Elmer Pyris 1, which is a power-compensated DSC. The samples were about 4 mm in diameter and 1 mm in height, which results in a sample mass of about 32 mg. The samples were placed on a plate of pure aluminium foil (5 mg) to prevent the micro furnace from element-diffusion. A double-stage mechanical cooler (Intracooler II) and pure nitrogen

as purge gas were used. To reach maximum cooling rates massive metal guard-ring inserts were attached (instead of the star shaped guard-ring inserts) to improve heat exchange between the ovens and the cold block. The block-temperature was −80 °C. The DSC is covered by a glove-box. This box was under slight over-pressure of dry air. Because of the dry-condition under the glove-box icing was reduced to a minimum. To avoid baseline drift problems sample- and baseline-measurements were done directly after each other.

Radiation losses play an important role for baseline stability in all DSCs. During the measurement, the alloyed samples are chang- ing their surface colour form bright to grey due to surface reactions. The change of surface colour is much stronger for the alloyed sam- ples than for the pure aluminium reference samples. Due to this surface-effect, the radiation behaviour is changing. Thereby the DSC-curves are bending. This bending can be strongly reduced by packing the samples in pure aluminium crucibles. At least in the Heat-Flow-DSCs crucibles are necessary to get a good accordance of sample- and baseline-measurement (Fig. 1).

However, also for the power-compensated DSC the curves are better reproduced with complete covering of the sample avoiding colour changes of the heat exchanging surfaces of the sample. The influence of colour changes on the measured heat-flow rates even for the nearly perfect three dimensional heat-flow rate sensor in a CALVET-type DSC is shown in Fig. 1.
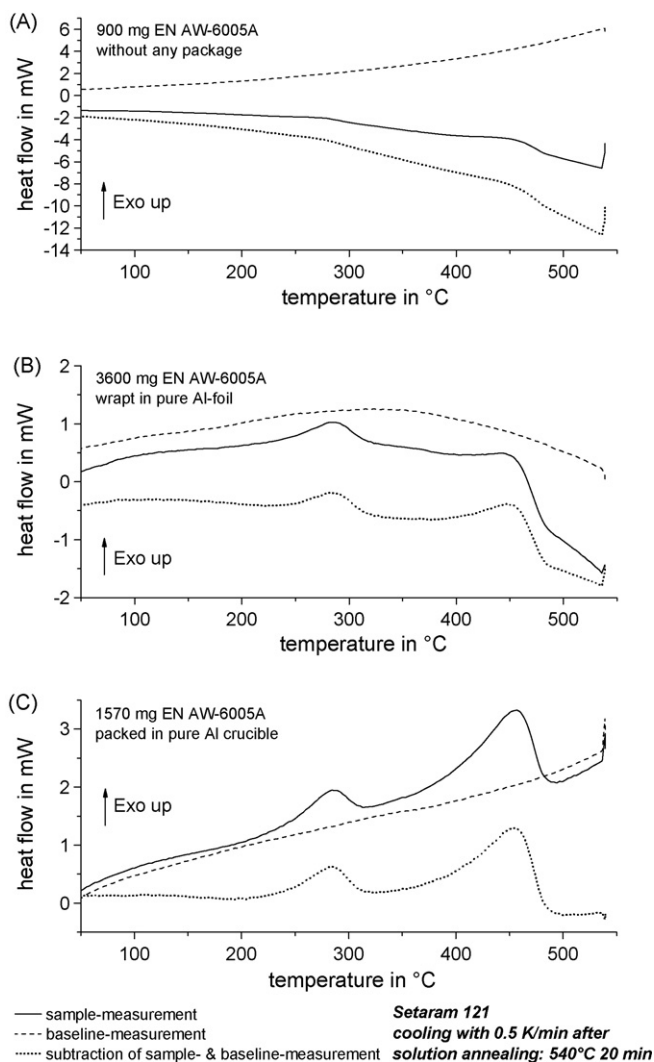
Fig. 1. Comparison of different sample-packing in the Heat-Flow-DSC of CALVET-type (Setaram 121); (A) no packing, (B) 40 mg pure Al-foil, and (C) 360 mg pure Al-crucible.
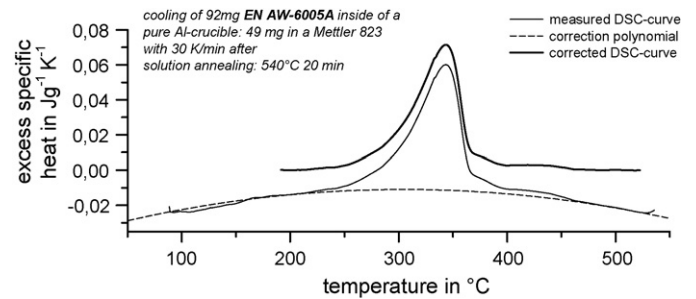
Fig. 2. Bending-correction with polynomial-function.

As mentioned above evaluation was done on the excess spe- cific heat capacity curves. To get these curves the heat-flow curves of a baseline-measurement (pure Al as sample and reference) was subtracted from the heat-flow curve of the appropriate sample- measurement and the start- and end-isotherms were aligned. The resulting curve was divided by sample mass and cooling rate as common to obtain excess specific heat capacity [17]. This was found by preliminary investigations to be the best way to resolve the precipitation reaction in the DSC signal on cooling.

Although it was tried to ensure optimal measurement condi- tions most curves were slightly bended. The curve bending changes continuously with changing cooling rate. Especially at high cool- ing rates, due to the tiny reactions, a highly scaled-up view of the DSC-curves was used for evaluation. Thereby the influence of curve bending on the relative evaluation error is increasing with increas- ing cooling rate. The commonly observed problems with curve bending at lower rates due to decreasing signal were avoided by choosing large sample masses and the appropriate calorimeter. The curve bending can be corrected with a polynomial curve of second- order (Fig. 2). In doing so, the error in integrating the peak-area was kept as small as possible.

The curves were evaluated for the characteristic temperatures of the reaction: start- and end-temperature but also for peak-area. The area under the peak(s) gives information about the released specific heat, which precisely is called "specific precipitation heat". This value is a measure for the amount of precipitates. With decreas- ing cooling rate the released specific precipitation heat approaches a limit: the equilibrium state. Under equilibrium or quasi-static con- ditions the alloying elements are precipitated according to the cor- responding phase diagram. This limiting specific precipitation heat can be used to estimate the amount of precipitates at higher rates as percentage of the quasi-static value. Under quasi-static conditions the precipitates are micron sized while at higher cooling rates they are mainly nanosized, see Fig. 8. Therefore size effects, e.g. surface energies, have to be taken into account for a correct determination of the amount of precipitates, which was not the aim of this study.

In some experiments at least two reactions overlap. The total precipitation heat measured is the sum of both released heats. For complete continuous cooling precipitation diagrams, a separation of the reactions is needed. Therefore, it was assumed that a single reaction causes a heat-peak that is shaped like a Gaussian distribu- tion curve. The measured excess specific heat capacity curves $c_p(T)$, were then approximated as a sum of two Gaussian peaks (Fig. 3).

For the evaluation of start- and end-temperatures defined points of the Gauss-curve were used:

$$c_p(T) = \left(\frac{\Delta h_1}{w_1 \sqrt{\pi/2}} \right) e^{-2\left(T - T_{\text{peak}\,1}/w_1\right)^2}$$

$$+ \left(\frac{\Delta h_2}{w_2 \sqrt{\pi/2}} \right) e^{-2\left(T - T_{\text{peak}\,2}/w_2\right)^2}$$
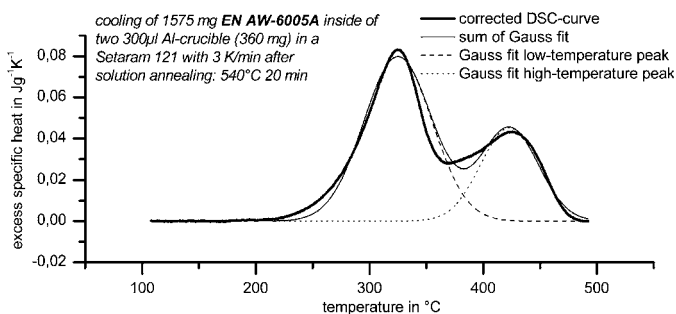
Fig. 3. Fit of the corrected excess specific heat capacity with two Gaussian curves.
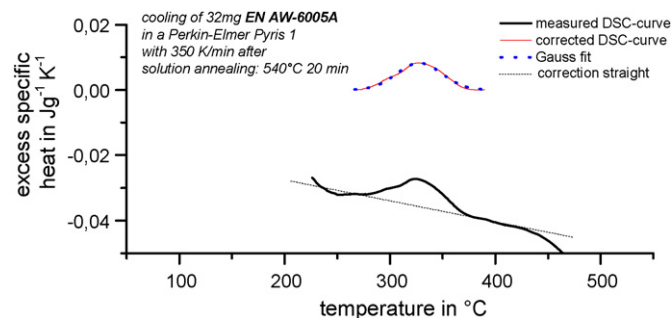
Fig. 4. Curve evaluation near critical cooling rate. T_{Start}: 371 °C; T_{End}: 285 °C; specific precipitation heat: 0.44 J/g.

with the two sets of fit parameters T_{peak}, peak-temperature; Δh, specific precipitation heat (peak-area) and w, width of the Gauss-curve.

Start- and end-temperatures of the peaks were defined as $T_{peak} \pm w$ respectively. They correspond to the points were the peak deviates for about 15% of the peak height from the baseline. Even the so calculated start- and end-temperatures of the reaction are not the real reaction start- and end-temperatures, this method offers an objective evaluation of the characteristic temperatures also in the region of overlapping peaks.

The amount of released heat decreases with increasing cooling rate. One aim of this study is the detection of the critical cooling rate at which the precipitation does not occur anymore. Therefore, an objective criterion is needed when no precipitation heat is detectable in the measured curves. The challenge is to decide when a precipitation peak is above the noise level. The detection limit was defined by the following criteria:

- the reaction is detectable in at least three repeated experiments,
- the reaction is detectable also at the next slower cooling rate,
- specific precipitation heat is at least 0.1 J/g,
- peak-temperatures are in the same region as for next slower rate.

One example of a curve evaluation near the detection limit is shown in Fig. 4. For correct curve interpretation, the evaluation must be done from slowest to faster cooling. Fig. 5 gives an overview over all cooling rates and thereby information about the peak-development. Additionally only with a general overview the curve bending can be corrected.

3. Results and discussion

Fig. 5 shows the bending-corrected excess specific heat curves for the aluminium wrought alloy 6005A during cooling after solution annealing at 540 °C for 20 min. These curves were measured with three different types of DSC-devices. Cooling rate ranges from
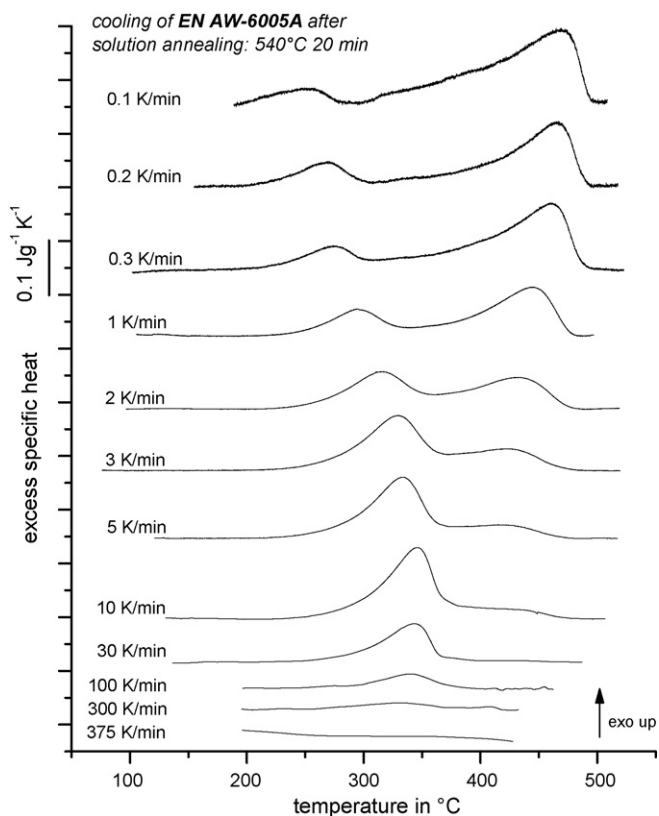
Fig. 5. Overview of bending-corrected curves from three different types of DSC-devices in a cooling rate region from 0.1 K/min to 375 K/min (0.1–5 K/min: Setaram 121; 10–30 K/min: Mettler 823; 100–375 K/min: Perkin-Elmer Pyris 1).

close to equilibrium conditions at 0.1 K/min to critical cooling rate, which was identified at 375 K/min in this case. Fig. 5 gives an overview of the peak-area and peak-temperature development. At the lowest cooling rate, close to equilibrium, the precipitation reaction starts at about 500 °C. Regarding the quasibinary phase-diagram Al–Mg_2Si [1], and estimating a Mg_2Si-content of 0.9 wt.% in the investigated composition of alloy 6005A, this start-temperature is nearly consistent with the solvus-temperature. At the cooling rate of 0.1 K/min two main peaks were identified: a high-temperature peak with peak-temperature of about 470 °C and a low-temperature peak with a peak-temperature of about 250 °C. The range between the peak-values is approximately 220 K. This precipitation temperature-range shortens with increasing cooling rate. Near the critical cooling rate of the high-temperature peak (30 K/min), the difference between the peak-values is only about 80 K (approximately: 340–420 °C). This shows increasing precipitation suppression with increasing cooling rate. At rates faster than 30 K/min only the low-temperature peak occurs. At rates equal or faster than 375 K/min, the precipitation is suppressed completely. The shift of the lower precipitation peak to higher temperatures with increasing cooling rate shows that thermal lag is not dominating the peak shifts observed.

Fig. 6 presents the full range continuous cooling precipitation diagram of EN AW-6005A. This diagram displays the investigated cooling curves in a graph of temperature as a function of time. The time axis is scaled logarithmic, causing the curved traces for cooling at constant rate. At 375 K/min (fat-dotted) there is no precipitation detectable any more hence this was identified as the critical cooling rate for the aluminium wrought alloy 6005A. On the cooling curves at slower cooling the start- and end-temperatures of the Gaussian peak-fit evaluation are inserted. In the range between 30 K/min down to about 1 K/min (corresponding to cooling times between
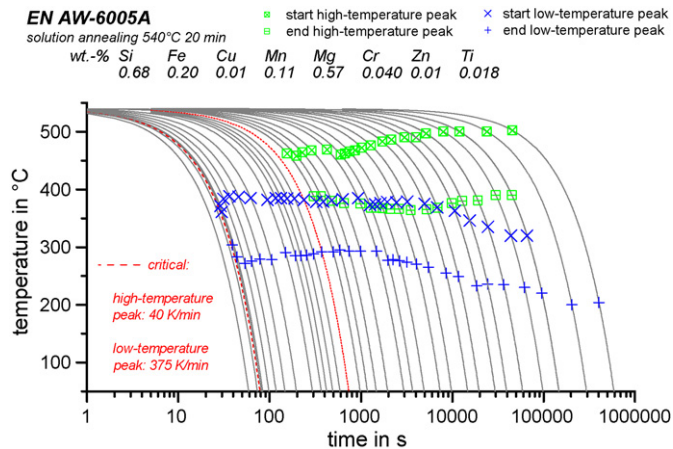
Fig. 6. Full range continuous cooling precipitation diagram of EN AW-6005A. The solid lines correspond to linear cooling in the range between 500 K/min and 0.5 K/min.

Fig. 7. Specific precipitation heat and Vickers-hardness (HV-1) after aging as a function of cooling rate. The displayed error bars show the uncertainty, which results from evaluation.

approximately 750 s and 20,000 s for the temperature-range from 540 to 50 °C) two Gaussian peaks fit the measured curves reasonable well. In the range of even slower cooling two Gaussian curves do not fit well the measured curves. The extreme slow curves show some indication for more than two reactions, see Fig. 5.

It must be mentioned, that the CCP-diagram is only valid for the investigated chemical composition, initial microstructure and solution annealing conditions. The large range between high-temperature peak and low-temperature peak indicates probably more than two reactions or at least highly asymmetric peaks. The two-peak fit is still used because more peaks/reactions were not identifiable for sure. In those cases with less correlation between the peak fit and the measured curve, the peak fit is done like that the sum of both peak areas agrees well to the integrated area of the measured curve. At the slowest cooling rate 0.05 K/min the lower limit of the DSCs used is reached. Because of the very small effects, the released heat due to the precipitation reaction is so small per time step that it is hardly detectable. Hence, the signal to noise ratio is bad.

The CCP-diagram in Fig. 6 delivers no information about the amount of released heat or the amount of precipitates respectively. This is shown in Fig. 7, which displays the released specific precipitation heat and the Vickers-hardness after artificial aging as function of cooling rate. The cooling rate axis is scaled decreasing logarithmic. This is done to allow an easy comparison with the time scale of the CCP-diagram.

From the peak-area determination, an uncertainty of about 10% is estimated. Additional the single areas of the double peak from the fits are displayed. There is a strong correlation between precipitation heat and hardness. If a precipitation occurs during cooling it is hardly possible to strengthen the material during the following aging process. At the slowest cooling the measured precipitation heat and the hardness approaches its saturation. This fact indicates that the equilibrium state is approached. Correlating the specific precipitation heat to the quasibinary phase-diagram Al–Mg$_2$Si, the equilibrium precipitation heat of about 11.5 J/g belongs to the amount of precipitated Mg$_2$Si which is nearly 0.9 wt.% for alloy 6005A. With this dependency the amount of precipitates can be approximated also for faster cooling. Because we do not know the (nano) size of the precipitates, which may affect the precipitation heat, we did not perform the calculation but an estimate is available from Fig. 7. At 10 K/min, for example, approximately 0.5 wt.% Mg$_2$Si are precipitated.

An additional confirmation of the DSC results is given by Fig. 8, which shows metallographic images of samples of aluminium alloy EN AW-6005A in different cooling conditions. The left picture shows a sample, which was cooled with 362 K/min—a rate near critical cooling rate. Therefore, precipitation during cooling is suppressed nearly completely. Visible is the light-grey aluminium matrix, but also some primary precipitates, which form already during the primary shaping and which are not changed by the age-hardening process. Energy dispersive X-ray (EDX)-analysis showed
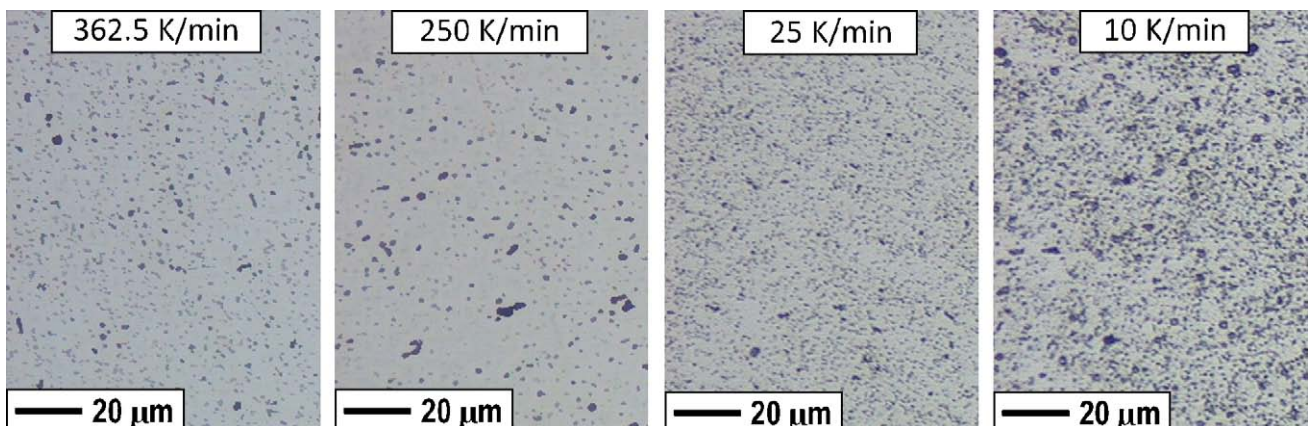
Fig. 8. Metallographic images of samples of EN AW-6005A: 540 °C 20 min, quenching: 362.5 K/min; 250 K/min; 25 K/min and 10 K/min; etching: 45 s with molybdenum acid (95 ml distilled H$_2$O + 5 ml HF + H$_2$MoO$_4$ supersaturated).

that those phases mainly contain Fe, Mn and Si. Those primary precipitates can be found at each cooling condition. The most right picture of Fig. 8 shows a sample, which was cooled at 10 K/min. At this rate, the amount of precipitates during cooling is about ten times larger than at 362 K/min. The precipitates, which are formed during slow cooling, have dimensions in the μm-range. EDX-analysis showed that the phases, which are affected by the cooling rate, mainly contain Mg and Si. With X-ray diffraction (XRD) the cubic structure of Mg_2Si could be detected at the slowest cooled sample.

Form the right picture to the left picture (increasing cooling rate) the amount of visible precipitates is decreasing significantly. This is also a visible expression of increasing precipitation suppression with increasing cooling rate.

4. Summary

For the aluminium–magnesium–silicon wrought alloy EN AW-6005A, age hardening was performed in three different types of Differential Scanning Calorimeters (DSC) whereby cooling rate varies over 3 orders of magnitude. For the used DSC-devices, optimal measurement conditions were found. Unavoidable remaining bending of the measured excess specific heat capacity curves was corrected.

When an aluminium alloy is solution annealed and afterwards cooled too slowly, an exothermal precipitation reaction occurs. With increasing cooling rate, the precipitation heat is decreasing. The influence of the cooling rate on the precipitation behaviour is described by continuous cooling precipitation diagrams. With this information, the quenching step of the age-hardening process can be optimized. Furthermore, simulation of precipitation processes during the quenching step of the age hardening is impossible without the material-data out of CCP-diagrams.

The complete CCP-diagram of EN AW-6005A has been recorded (Fig. 6). The critical cooling rate, which is the minimum cooling rate, at which no precipitation heat is detectable, was determined. For the investigated alloy EN AW-6005A the critical cooling rate equals 375($\pm$10) K/min. The definition of precipitation start- and end-temperatures was done by fitting the measured precipitation peaks by Gaussian peaks. Defined points of the Gauss-curves were used to evaluate the characteristic temperatures. In the cooling rate range from 375 K/min to 40 K/min, only one reaction is detectable. At slower cooling rates there are at least two reactions detectable. In this region, the peak fit is done with two Gaussian peaks, which gave a good fit in the range between 30 K/min and about 1 K/min. The characteristic temperatures could be detected with an accuracy of $\pm$10 K. The challenge of the needed decision between thermal noise and occurrence of a reaction-peak near the critical cooling rate has been overcome by well-defined decision criteria. The amount of released heat could be determined with an uncertainty of about 10%. The DSC results are well confirmed by hardness testing and metallographic images.

An open question is the identification of the single precipitates for overlapping peaks. Therefore, electron-microscopically analyses will be necessary to get information about the quantity of precip-

itates, their locations in the grain structure and their composition. First results indicate the presence of Mg_2Si.

With the used DSC-devices, precipitation reactions are detectable in a range of cooling rates between 0.1 K/min and some hundred K/min. It is intended to record CCP-diagrams for other aluminium alloys too. Therefore, higher cooling rates could be necessary. Scanning calorimetry is possible with cooling rates up to 1 MK/s nowadays [9,10]. With the device used by Gao et al. [11] the gap in heating and cooling rates between ultrafast and conventional DSC is closed. Appropriate calorimeters are available, but they have to be adjusted to the specific problem.

References

[1] I.J. Polmear, Ligth Alloys, Butterworth-Heinemann, Oxford, 2006.
[2] T. Herding, O. Kessler, F. Hoffmann, P. Mayr, An approach for Continuous Cooling Transformation (CCT) diagrams of aluminium alloys, in: P.J. Gregson, S.J. Harris (Eds.), 8th International Conference on Aluminium Alloys, Trans Tech Publications Ltd, Cambridge, UK, 2002, pp. 869–874.
[3] O. Kessler, R. von Bargen, F. Hoffmann, H.W. Zoch, Continuous cooling transformation (CCT) diagram of aluminum alloy Al–4.5Zn–1Mg, in: W.J. Poole, M.A. Wells, D.J. Lloyd (Eds.), 10th International Conference on Aluminium Alloys 2006, Pts 1 and 2, Trans Tech Publications, 2006, pp. 1467–1472.
[4] B. Milkereit, O. Kessler, C. Schick, Continuous cooling precipitation diagrams of aluminium–magnesium–silicon alloys, in: J. Hirsch, B. Skrotzki, G. Gottstein (Eds.), 11th International Conference on Aluminium Alloys, Deutsche Gesellschaft für Materialkunde e.V., WILEY-VCH Weinheim, Aachen, Germany, 2008, pp. 1232–1237.
[5] R. von Bargen, Kontinuierliche Zeit-Temperatur-Ausscheidungsdiagramme der Aluminiumlegierungen 7020 und 7050, Härterei-Technische Mitteilungen 62(6) (2007).
[6] J.L. Cavazos, R. Colas, Quench sensitivity of a heat treatable aluminum alloy, Mater. Sci. Eng. A: Struct. Mater. Properties Microstruct. Process. 363 (1–2) (2003) 171–178.
[7] H.Y. Li, J.F. Geng, Z.Q. Zheng, C.J. Wang, Y. Su, B. Hu, Continuous cooling transformation curve of a novel Al–Cu–Li alloy, Trans. Nonferrous Met. Soc. China 16 (5) (2006) 1110–1115.
[8] E. Calvet, H. Prat, H. Skinner, Recent Progress in Microcalorymetry, Pergamon Press, Oxford, London, New York, Paris, 1963.
[9] S.A. Adamovsky, A.A. Minakov, C. Schick, Scanning microcalorimetry at high cooling rate, Thermochim. Acta 403 (1) (2003) 55–63.
[10] A.A. Minakov, C. Schick, Ultrafast thermal processing and nanocalorimetry at heating and cooling rates up to 1 MK/s, Rev. Sci. Instrum. 78 (7) (2007) 073902.
[11] Y.L. Gao, E. Zhuravlev, C.D. Zou, B. Yang, Q.J. Zhai, C. Schick, Calorimetric measurements of undercooling in single micron sized SnAgCu particles in a wide range of cooling rates, Thermochim. Acta 482 (1–7) (2008).
[12] S. Esmaeili, X. Wang, D.J. Lloyd, W.J. Poole, On the precipitation-hardening behavior of the Al-Mg-Si-Cu, Metall. Mater. Trans. A: Phys. Metall. Mater. Sci. 34A (3) (2003) 751–763.
[13] A. Gaber, A.M. Ali, K. Matsuda, T. Kawabata, T. Yamazaki, S. Ikeno, Study of the developed precipitates in Al-0.63Mg-0.37Si-0.5Cu (wt.%) alloy by using DSC and TEM techniques, J. Alloy. Compd. 432 (1–2) (2007) 149–155.
[14] M. Vedani, G. Angella, P. Bassani, D. Ripamonti, A. Tuissi, DSC analysis of strengthening precipitates in ultrafine Al-Mg-Si alloys, Springer, 2007, pp. 277–284.
[15] X. Wang, S. Esmaeili, D.J. Lloyd, The sequence of precipitation in the Al-Mg-Si-Cu alloy AA6111, Metall. Mater. Trans. A: Phys. Metall. Mater. Sci. 37A (9) (2006) 2691–2699.
[16] M.J. Starink, Analysis of aluminium based alloys by catorimetry: quantitative analysis of reactions and reaction kinetics, Int. Mater. Rev. 49 (3–4) (2004) 191–226.
[17] W. Hemminger, G.W.H. Höhne, Grundlagen der Kalorimetrie, Akademie-Verlag, Berlin, 1980.
[18] A. Deschamps, G. Texier, S. Ringeval, L. Delfaut-Durut, Influence of cooling rate on the precipitation microstructure in a medium strength Al–Zn–Mg alloy, Mater. Sci. Eng. A: Struct. Mater. Properties Microstruct. Process. 501 (1–2) (2009) 133–139.